Coupled Analysis of Residual Soil Slope subjected to Rainfall

Krishna M. Neaupane and Ahmed Faazal
Sirindhorn International Institute of Technology, Thammasat University
Klong Luang, Pathumthani 12121, Thailand
Phone (66-2) 986 – 9009 ext. 1911
Fax (66-2) 986 – 9009 ext. 1905
E-mail: krishna@siit.tu.ac.th

Abstract

A residual soil slope is under investigation using a coupled mechanistic approach. The numerical code, DEFLOC (DEformation FLOw Coupled program), has been developed in the MATLAB environment that takes into account the basics of unsaturated soil behavior. Two-dimensional numerical modeling was performed based on the Galerkin's method applied to poro-elasticity. The effects of hydraulic characteristics, matric suction and degree of saturation on the pore pressure and deformation behavior of a residual soil slope under rainfall were investigated. The results reveal a typical process of infiltration into unsaturated soil slopes.

1. Introduction

Rainfall-triggered slope failures are the most common slope instability phenomenon in unsaturated residual soils along the monsoon affected areas of South Asia and South East Asia [1, 2]. Such failures occur on both virgin and construction modified hill slopes on the northern and north eastern part of Thailand during rainy season. The hillslopes are generally covered with unsaturated residual soil and often shallow earth slips are predominant accounting for about 80 % of failures [3]. In general, the failures on unsaturated soil occur due to an increase in moisture content and a decrease in matric suction. Wetting reduces the additional shear strength provided by the matric suction and causes the failure [4]. A rise in the groundwater level also increases the moisture and unit weight content of soil, thereby reducing the resisting force and increasing the driving moment.

The behavior of partially saturated soils can be very different to that of fully saturated and dry soils. For many geotechnical problems involving unsaturated soils, knowledge of the porewater pressures, the negative porewater pressure in particular, is of primary importance. The effect of negative porewater pressure (matric suction) on flow-deformation regime can not be overlooked where the concern is a shallow failure surface [5].

A fully coupled flow-deformation system is characterized by the procedure that rigorously incorporates the interactions among the three bulk phases of a deforming porous medium, and therefore, fluid flow and mechanical equilibrium equations are required to be solved simultaneously. In case of an uncoupled analysis, a solution to the flow equation is first used to determine the pore pressure changes in a given time step, and pore-pressure changes are then used as applied loads in a deformation analysis. The fluid flow and deformation analyses are carried out separately. The issue of coupling versus uncoupling in consolidation type problems has been previously addressed by several researchers [6-8]. As pointed out by Desai and Saxena [9] and Lewis et al. [10] coupling is generally accepted when the forcing function is applied to the displacement field, e.g. by a physical load or a foundation pressure. The response of unsaturated soils subjected to rainfall perturbations (forcing function), therefore, is described in this research with a coupled flow – deformation analysis.

Several attempts have been made to simulate multiphase flow in deforming porous media based on the theory of poroelasticity. However, only a few fully coupled models of multiphase flow in a deforming porous medium are available due to the complexities. Although the existing models are capable of reproducing some of the important behavior of partially saturated soils, most models are basic, and impose limitations because they do not consider down-slope flows, rainfall intensity, and most importantly, the dependence of soil permeability on moisture content [11-13].

An analytical solution for a coupled problem in unsaturated soil is not possible without making several simplifying assumptions. However, attempts have been made, in recent years, to come up with the closed form solution of the governing equations of unsaturated soils, including equilibrium equations and continuity flow equations [14]. Nevertheless, the numerical solution becomes indispensable for such a complex problem of investigating the behavior of partially saturated soils.

This research aims at modeling the flow deformation behavior of the unsaturated soil subjected to rainfall using a coupled numerical code, DEFLOC (DEformation FLOw Coupled program). The finite element program developed in the MATLAB environment takes into account the basic features of unsaturated soil behavior.

2. Theoretical Backgrounds

Early attempts to describe the behavior of partially saturated soils made the assumption that the effective stress principle is applicable to such soils, and that the mechanical behavior can be fully described in the conventional (q, p') stress space. Generalized effective stress expressions were proposed to include partially saturated soils into the conventional soil mechanics framework, the best known being that proposed by Bishop [15]. The Bishop's approach proved capable of reproducing some behaviors of partially saturated soils, such as the shear strength increase due to suction, but could not explain others, such as wetting induced collapse. It is now generally accepted that two independent stress variables are necessary in order to explain the behavior of partially saturated soils. Bishop and Blight [16] first used net total stress $(\sigma - p_a)$ and suction $(p_a - p_w)$ to investigate the volumetric and strength behavior of partially saturated soils and produced graphical representations of state surfaces and failure envelopes. Researchers suggest that any pair of stress state variables among the following: $(\sigma - p_a)$, $(\sigma - p_w)$ and $(p_a - p_w)$ can be adopted when describing partially saturated soil behavior [17]. The most commonly used pair is net total stress $(\sigma_w - p_a)$ and suction $(p_a - p_w)$ [17, 18].

3. Mathematical Formulation

Balanced Equations

Water Mass Balance Equation

The water mass balance equation for unsaturated soil is:

$$\frac{\partial(\rho_w n S_r)}{\partial t} + \mathrm{div}(\rho_w \mathbf{v}_w) = 0 \qquad (1)$$

where ρ_w is the density of water, n is porosity, S_r is the degree of saturation, and $\mathbf{v_w}$ is the velocity of water. Density of water is assumed to be constant, and hence a weak formulation of Eq (1), after taking arbitrary volume integral and limiting the scope for two-dimensional problems, gives rise to:

$$\int_A \mathbf{N}_\mathbf{n}^\mathrm{T} \frac{\partial}{\partial t}(n S_r)\, dA + \int_\Gamma \mathbf{N}_\mathbf{n}^\mathrm{T} q_w\, d\Gamma - \int_A \mathbf{B}_\mathbf{n}^\mathrm{T} \mathbf{v}_w\, dA = 0 \qquad (2)$$

in which the term q_w, is the water flux across the boundary given by: $q_w = \mathbf{v}_\mathbf{w}^\mathbf{T}\mathbf{n}$. Water flow is described by a generalization of Darcy's law: $\mathbf{v}_\mathrm{w} = -K_w \nabla\left(p_w/\gamma_w + z\right)$, where K_w is the coefficient of permeability, z the elevation head and γ_w the specific weight of water (assumed constant). Jacquard [19] proposed a relationship for coefficient of permeability, K_w, in terms of suction as $K_w = A_w K_{ws} \Big/ \left\{A_w + \left(C_w\left(p_a - p_w\right)\right)^{B_w}\right\}$ where A_w, B_w, C_w and K_{ws} are constants. In unsaturated flow, the hydraulic conductivity is highly dependent on the water content of the soil. Only when the soil approaches saturation, does the hydraulic conductivity become constant. Numerical models have been proposed to represent the permeability in a variety of functional forms, e.g. in terms of matric suction or degree of saturation or volumetric water content. Lu and Likos presented a summary of empirical and macroscopic equations for modeling unsaturated hydraulic conductivity functions in a tabular form [20]. Among several numerical models, Bourgeois [21] equation gives relationship between degree of saturation and matric suction as described by:

$$S_r = S_{ri} + A_w\left(S_{rs} - S_{ri}\right) \Big/ \left\{A_w + \left(C_w\left(p_a - p_w\right)\right)^{B_w}\right\} \quad (3)$$

where A_w, B_w, C_w, S_{rs} and S_{ri} are constants. In soil problems, an increase in suction is accompanied by a decrease in the degree of saturation, and a decrease in the suction results in an increase in the degree of saturation, ultimately approaching to one (saturated condition). For isotropic conditions, Lloret and Alonso [22] suggested state surface as:

$$\begin{aligned} e = {} & d + a\left(\sigma - p_a\right) + b\left(p_a - p_w\right) \\ & + c\left(\sigma - p_a\right)\left(p_a - p_w\right) \end{aligned} \quad (4)$$

where a, b, c and d are constants, and e being the void ratio. Equation (2) is simplified into the weak form:

$$\mathbf{C}_1^1 \frac{\partial}{\partial t}\left(\overline{\mathbf{p}_\mathrm{w}}\right) + \mathbf{C}_1^2 \frac{\partial}{\partial t}\left(\overline{\mathbf{u}}\right) + \mathbf{C}_1^3 + \mathbf{C}_1^4 \overline{\mathbf{p}_\mathrm{w}} + \mathbf{C}_1^5 = 0 \quad (5)$$

in which the integrals $\mathbf{C}_1^1$, $\mathbf{C}_1^2$, $\mathbf{C}_1^3$, $\mathbf{C}_1^4$ and $\mathbf{C}_1^5$ are described in Table 1.

Air Mass Balance Equation

The continuity of air mass filling the soil void is given by:

$$\frac{\partial}{\partial t}\left[\rho_a n\left(1 - S_r + HS_r\right)\right] + \mathrm{div}\left[\rho_a\left(\mathbf{v}_\mathrm{a} + H\mathbf{v}_\mathbf{w}\right)\right] = 0 \quad (6)$$

It is assumed that air behaves as an ideal gas, and hence density and pressure are related by: $\rho_a = \left(M/RT\right)p_a$, where T (K) is the absolute temperature, R the gas constant, M the molecular weight of air. Similarly, the motion of air can be described by a generalization of Darcy's law: $\mathbf{v}_\mathrm{a} = -K_a \nabla\left(p_a/\gamma_a + z\right)$, where K_a is the coefficient of permeability, and γ_a the specific weight of air. Brun proposed a relationship for the coefficient of air permeability in terms of suction as: $K_a = A_a K_{as} \Big/ \left\{A_a + \left(C_a\left(p_a - p_w\right)\right)^{-B_a}\right\}$, where A_a, B_a, C_a and K_{as} are constants [23]. The weak formulation of Eq (6) reduces to the form of:

$$\begin{aligned} & \mathbf{C}_3^1 \frac{\partial}{\partial t}\left(\overline{\mathbf{u}}\right) + \mathbf{C}_3^2 \frac{\partial}{\partial t}\left(\overline{\mathbf{p}_\mathbf{a}}\right) + \mathbf{C}_3^3 \frac{\partial}{\partial t}\left(\overline{\mathbf{p}_\mathbf{w}}\right) \\ & + \mathbf{C}_3^4 \overline{\mathbf{p}_\mathbf{a}} + \mathbf{C}_3^5 \overline{\mathbf{p}_\mathbf{w}} + \mathbf{C}_3^6 + \mathbf{C}_3^7 = 0 \end{aligned} \quad (7)$$

Momentum Equation

The general momentum balance equation can be written as:

$$\tilde{\nabla}^{\mathrm{T}}\boldsymbol{\sigma} + \mathbf{b} = 0 \tag{8}$$

where $\boldsymbol{\sigma}$ is the total stress, and $\mathbf{b}$ the body forces. For this particular problem, the body force is due to gravity only and it is taken upward positive. Total stress in Eq. (8) can be expressed in terms of effective stress using Bishop's relationship as: $\boldsymbol{\sigma}^{*} = (\boldsymbol{\sigma} - \mathbf{m}p_a) + \chi(\mathbf{m}p_a - \mathbf{m}p_w)$, where χ is a function of the degree of saturation, p_a is the pore air pressure, and p_w is the pore water pressure [15]. The well known Bishop's parameter (χ) can be expressed as a function of degree of saturation or volumetric water content as:

$$\chi = \frac{\theta - \theta_r}{\theta_s - \theta_r} = \frac{S_r - S_{ri}}{1 - S_{ri}} \; ; \; 0 \le \chi \le 1 \tag{9}$$

where θ_s, and θ_r represent saturated and residual water contents, respectively, and S_{ri} is residual degree of saturation [24]. The nature of $\mathbf{m}$ implies that the fluid pressure only effect the normal stress components. Expressing strain in terms of displacement, the discretized moment degenerated equation is reduced to:

$$\begin{aligned}\left(\mathbf{C}_2^1 - \mathbf{C}_2^2\right)\frac{\partial}{\partial t}\overline{\mathbf{p}_\mathbf{a}} + \mathbf{C}_2^2\frac{\partial}{\partial t}\overline{\mathbf{p}_\mathbf{w}} + \mathbf{C}_2^3\frac{\partial}{\partial t}\overline{\mathbf{u}} \\ = \mathbf{C}_2^4 + \mathbf{C}_2^5 + \mathbf{C}_2^6\end{aligned} \tag{10}$$

4. Governing Equations

The three equilibrium equations are now combined to perform a coupled analysis of the system. The stress-strain relationship was described by using non-linear elastic model based on Hooke's law. The unknowns are pore pressure and deformation. The equations in incremental Galerkin's formulation are given in matrix as:

$$\begin{bmatrix} \mathbf{C}_3^2 & \mathbf{C}_3^3 & \mathbf{C}_3^1 \\ 0 & \mathbf{C}_1^1 & \mathbf{C}_1^2 \\ \left(\mathbf{C}_2^1 - \mathbf{C}_2^2\right) & \mathbf{C}_2^2 & \mathbf{C}_2^3 \end{bmatrix} \times \frac{\partial}{\partial t}\begin{Bmatrix} \overline{\mathbf{p}_\mathbf{a}} \\ \overline{\mathbf{p}_\mathbf{w}} \\ \overline{\mathbf{u}} \end{Bmatrix} + \begin{bmatrix} \mathbf{C}_3^4 & \mathbf{C}_3^5 & 0 \\ 0 & \mathbf{C}_1^4 & 0 \\ 0 & 0 & 0 \end{bmatrix} \times \begin{Bmatrix} \overline{\mathbf{p}_\mathbf{a}} \\ \overline{\mathbf{p}_\mathbf{w}} \\ \overline{\mathbf{u}} \end{Bmatrix} = \begin{Bmatrix} -\mathbf{C}_3^6 - \mathbf{C}_3^7 \\ -\mathbf{C}_1^3 - \mathbf{C}_1^5 \\ \mathbf{C}_2^4 + \mathbf{C}_2^5 + \mathbf{C}_2^6 \end{Bmatrix} \tag{11}$$

Table 1: Integrals described in Eqs. (5), (7), (11)

Water mass balance equations	
$\mathbf{C}_1^1 = \int_A \mathbf{N}_\mathbf{n}^{\mathrm{T}} n \frac{\partial S_r}{\partial p_w} \mathbf{N}_\mathbf{n} \, dA$	
$\mathbf{C}_1^2 = \int_A \mathbf{N}_\mathbf{n}^{\mathrm{T}} S_r \mathbf{m}^{\mathrm{T}} \mathbf{B}_\mathbf{m} \, dA$	
$\mathbf{C}_1^3 = \oint_\Gamma \mathbf{N}_\mathbf{n}^{\mathrm{T}} q_w \, d\Gamma$	
$\mathbf{C}_1^4 = \int_A \frac{1}{\gamma_w} \mathbf{B}_\mathbf{n}^{\mathrm{T}} K_w \mathbf{B}_\mathbf{n} \, dA$	
$\mathbf{C}_1^5 = \int_A \mathbf{B}_\mathbf{n}^{\mathrm{T}} K_w \nabla z \, dA$	
Air mass balance equations	
$\mathbf{C}_3^1 = \int_A \mathbf{N}_\mathbf{n}^{\mathrm{T}} \mathbf{N}_\mathbf{n} \overline{\mathbf{p}_\mathbf{a}} \mathbf{m}^{\mathrm{T}} \mathbf{B}_\mathbf{m} \, dA + (H-1) \int_A \mathbf{N}_\mathbf{n}^{\mathrm{T}} p_a S_r \mathbf{m}^{\mathrm{T}} \mathbf{B}_\mathbf{m} \, dA$	
$\mathbf{C}_3^2 = \int_A \mathbf{N}_\mathbf{n}^{\mathrm{T}} n \mathbf{N}_\mathbf{n} \, dA + (H-1) \int_A \mathbf{N}_\mathbf{n}^{\mathrm{T}} \left(\mathbf{m}^{\mathrm{T}} \mathbf{B}_\mathbf{m} \mathbf{u}\right) S_r \mathbf{N}_\mathbf{n} \, dA$	
$\mathbf{C}_3^3 = (H-1) \int_A \mathbf{N}_\mathbf{n}^{\mathrm{T}} \mathbf{N}_\mathbf{n} \overline{\mathbf{p}_\mathbf{a}} n \frac{\partial S_r}{\partial p_w} \mathbf{N}_\mathbf{n} \, dA$	
$\mathbf{C}_3^4 = \int_A \frac{1}{\gamma_a} \mathbf{B}_\mathbf{n}^{\mathrm{T}} \mathbf{N}_\mathbf{n} \overline{\mathbf{p}_\mathbf{a}} K_a \mathbf{B}_\mathbf{n} \, dA$	
$\mathbf{C}_3^5 = \int_A \frac{1}{\gamma_w} \mathbf{B}_\mathbf{n}^{\mathrm{T}} H p_a K_w \mathbf{B}_\mathbf{n} \, dA$	
$\mathbf{C}_3^6 = \oint_\Gamma \mathbf{N}_\mathbf{n}^{\mathrm{T}} \mathbf{N}_\mathbf{n} \overline{\mathbf{p}_\mathbf{a}} q_a \, d\Gamma + \oint_\Gamma \mathbf{N}_\mathbf{n}^{\mathrm{T}} H \mathbf{N}_\mathbf{n} \overline{\mathbf{p}_\mathbf{a}} q_w \, d\Gamma$	
$\mathbf{C}_3^7 = \int_A \mathbf{B}_\mathbf{n}^{\mathrm{T}} \mathbf{N}_\mathbf{n} \overline{\mathbf{p}_\mathbf{a}} K_a \nabla z \, dA + \int_A \mathbf{B}_\mathbf{n}^{\mathrm{T}} H \mathbf{N}_\mathbf{n} \overline{\mathbf{p}_\mathbf{a}} K_w \nabla z \, dA$	
Momentum equations	
$\mathbf{C}_2^1 = \int_A \mathbf{B}_\mathbf{m}^{\mathrm{T}} \mathbf{m} \mathbf{N}_\mathbf{n} \, dA$	$\mathbf{C}_2^4 = \oint_\Gamma \mathbf{N}_\mathbf{m}^{\mathrm{T}} \frac{\partial}{\partial t} \mathbf{t} \, d\Gamma$
$\mathbf{C}_2^2 = \int_A \mathbf{B}_\mathbf{m}^{\mathrm{T}} \chi \mathbf{m} \mathbf{N}_\mathbf{n} \, dA$	$\mathbf{C}_2^5 = \int_A \mathbf{N}_\mathbf{m}^{\mathrm{T}} \frac{\partial}{\partial t} \mathbf{b} \, dA$
$\mathbf{C}_2^3 = \int_A \mathbf{B}_\mathbf{m}^{\mathrm{T}} \mathbf{D} \mathbf{B}_\mathbf{m} \, dA$	$\mathbf{C}_2^6 = \int_A \mathbf{B}_\mathbf{m}^{\mathrm{T}} \mathbf{D} \frac{\partial}{\partial t} \boldsymbol{\varepsilon}_\mathbf{0} \, dA$

5. Application of Model

A soil-slope problem in residual soil is taken for the demonstration. The rainfall perturbation is taken as the forcing function that affects the flow regime as well as soil deformation. The displacement boundary conditions and slope dimensions are displayed in the Fig. 1. No flow boundary is assumed on either side of the slope (*af*, *de* and *fe*). Material properties input are shown in Table 2. Rainfall intensity of 20 mm/hr is applied to surfaces *ab*, *bc* and *cd* of the slope. For the slope in residual soil, pore-air pressure is assumed to be zero. Initial water pressure is illustrated in Fig. 2 as a contour plot. At water table, pore pressure is zero, and it become negative upwards, positive downwards as computed by: $P_w = \pm(\rho \cdot g \cdot h)$, where ρ is the density of water, g is the acceleration due to gravity and h is the height at which pore pressure is computed. The results from the code, with rainfall infiltration for 24 hours, are presented here.

Table 2: Material Properties

Water permeability	$K_{ws} = 5\times10^{-5}$ (m/s), $A_w = 1.0$, $B_w = 0.96$, $C_w = 5.16\times10^{-4}$
Degree of saturation	$S_{ri} = 0.08$, $S_{rs} = 1.0$, $A_w = 0.96$, $B_w = 3.5$, $C_w = 5.00\times10^{-5}$
Void ratio – state surface	$A = -7.58\times10^{-8}$, $b = -6.45\times10^{-8}$, $c = 1.61\times10^{-10}$, $d = 0.6462$
Young's modulus	$E = 7.88\times10^{9}$ N/m^3
Poisson's ratio	$\mu = 0.35$
Rainfall intensity	20 mm/hr

6. Results and Discussion

With the Dirichlet boundary condition on the nodes of the boundary *'ed'* when the water flows into slope, and Neuman Boundary condition (impervious boundary) when the water begins to discharge from the slope, contours of developed pore pressure is plotted as shown in Fig. 3. Induced deformation at the end of 24 hours of consistent rainfall is presented in Fig. 4 as a vector diagram. As expected the arrowheads of the diagram point to the slope toe professing a impending slope failure.

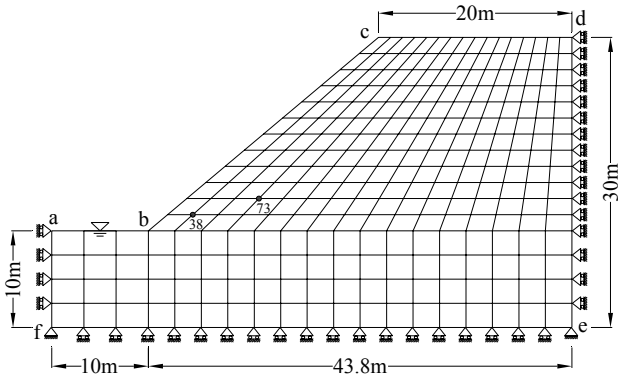

Figure 1: Domain of Analysis

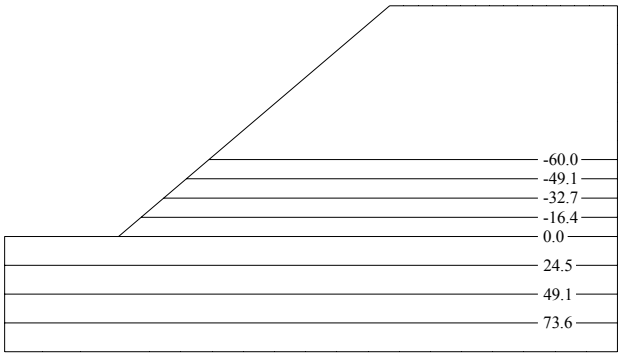

Figure 2: Contour lines of initial pore-pressure (in kPa)

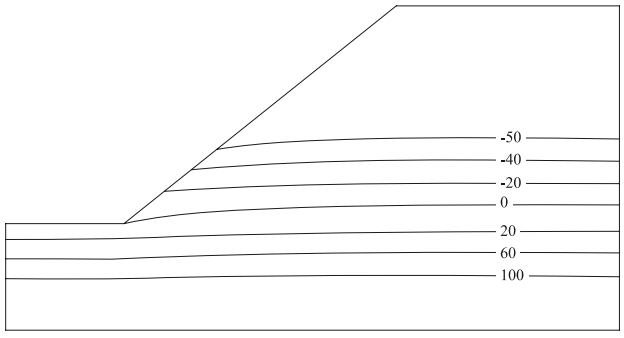

Figure 3: Contour lines of pore-pressure after 24 hours of rainfall (in kPa)

Results from the infiltration induced changes in matric suction are presented in Figs 5 and 6. Two nodes (node 38 and 73) were carefully selected to describe the effects of infiltration. Node 38 is close to the slope toe which could be affected by accumulation of flow whereas the node 73 is 4 m behind the slope. The matric suction decreases with time due to infiltration and eventually converges towards zero.

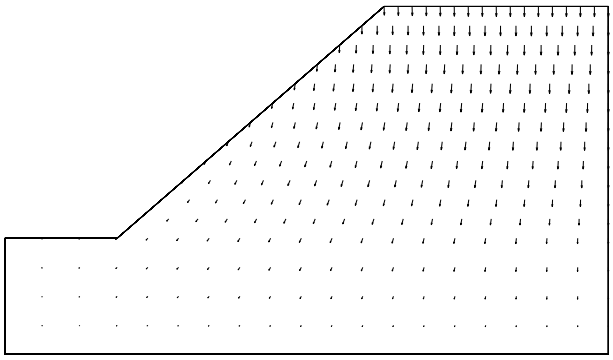

Figure 4: Deformation vectors at 24 hrs

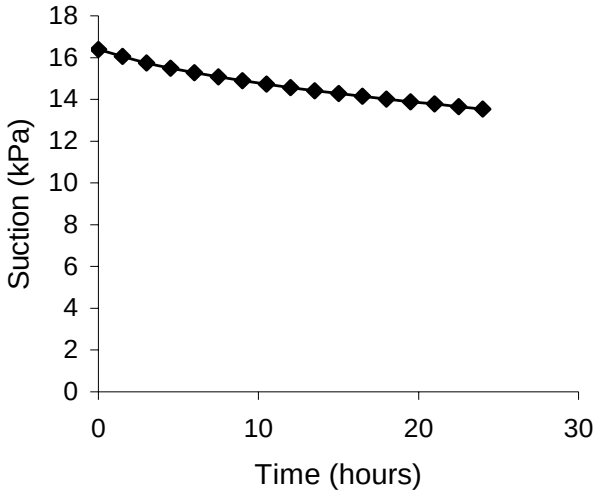

Figure 5: Time histories of suction at node 38

The response is different depending upon the distance from the slope surface and initial conditions of water pressure at the nodes. For the node closer to the surface (node 38), the reduction in matric suction starts immediately, whereas for the node 73, matric suction remains constant until 8 hours of consistent rainfall and drops rapidly, as shown in Fig. 6 as it takes more time for the seeping rainwater to reach a deep place.

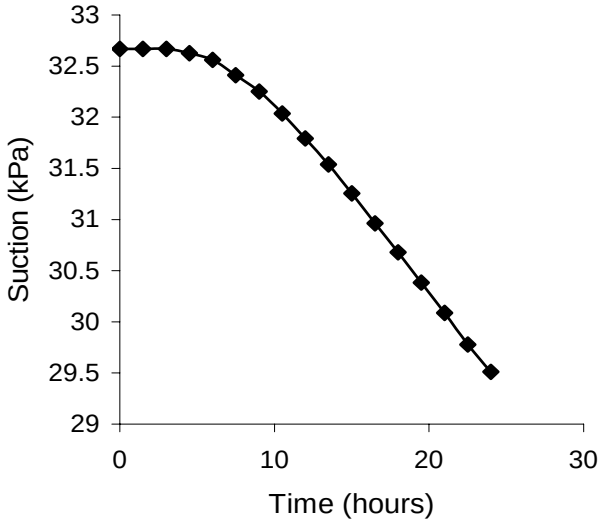

Figure 6: Time histories of suction at node 73

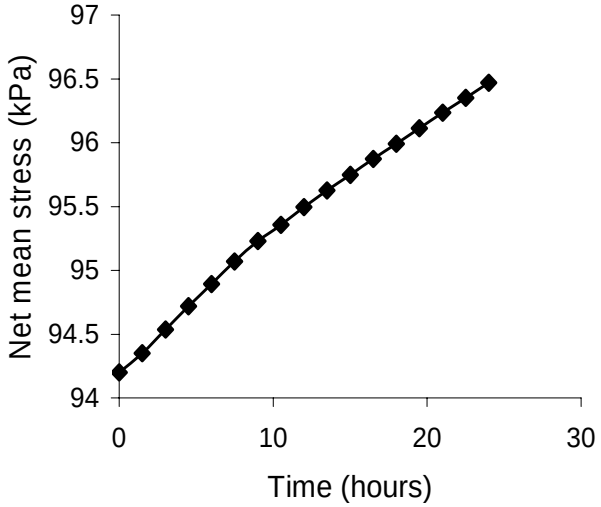

Figure 7: Time histories of net mean stress at node 38

The time histories of net mean stress are given in Figs. 7 and 8. The increase in net mean stress with time as presented in the Figures can be attributed to the increase in unit weight of soil due to increase of moisture content. As the infiltration continues, the net mean stress should

stabilize as the soil becomes saturated, and the net stress becomes the effective stress as described by Terzaghi's effective stress equation.

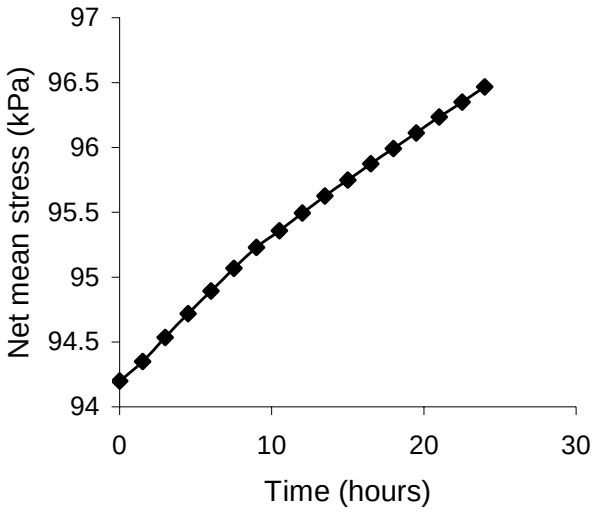

Figure 8: Time histories of net mean stress at node 73.

7. Conclusions

Numerical analysis plays an important role in the investigation of the behavior of partially saturated soils by highlighting aspects which are important in engineering practice, and illustrating the effect of partial soil saturation on the behavior of geotechnical structures. In this connection, the finite element model was developed, and the numerical simulation was performed on the formulations taking into account the basics of unsaturated soil behavior to a slope problem in residual soil subjected to rainfall. The response of the soil slope to rainfall perturbation was studied using time histories of matric suction, net mean stress and deformation. It was revealed that the matric suction reduced immediately closer to the slope surface, but took more time for the seeping rainwater to reach a deeper place. Likewise, the net mean increased due to the increase of moisture content. However, the current study uses non-linear elastic model based on Hooke's law. Therefore, it is reasonable to continue the analyses only up to the stage where the slope failure does not occur. Further development is, therefore, required to describe the mechanical response of unsaturated soil with nonlinear elasto-plastic formulation.

NOTATION

σ, $\boldsymbol{\sigma}^*$	Total stress, Effective stress vector
p_w, p_a	Pore water , Pore air pressure
S_r	Degree of saturation
$\mathbf{v_w}$, $\mathbf{v_a}$	Velocity of water, Velocity of air
q_w	Water flux
ρ_w, γ_w	Density/unit weight of water
z	Elevation head
K_w	Coefficient of permeability
K_{ws}, A_w, B_w, C_w	Model parameters for permeability
S_{ri}, A_w, B_w, C_w	Model parameters for saturation
a, b, c, d	Parameters for state-surface model
H	Henry's coefficient
χ	Bishop's parameter

References

[1] Neaupane, K.M., Piantanakulchai, M. (2006). Analytic network process model for landslide hazard Zonation. Engineering Geology, 85:281–294.

[2] Singh, V.K., Lukmuang, M., Glawe, U. (2003). Observations on landslides resulting from extreme rainfalls in the NE of Thailand (Phu Rua District, Loei Province. In:Int. Conf. Slope Eng. University of Hongkong, Hongkong Vol. 1, pp 203–207.

[3] Asian Disaster Preparedness Center (ADPC), (2006). Rapid assessment: Flashflood and landslide disaster in the provinces of Uttaradit and Sukhothai northern Thailand. Urban Disaster Management, ADPC, Thailand.

[4] Krahn, J., Fredlund, D.G., Klassen, G.M., (1989). Effect of soil suction on slope stability at notch hill. Canadian Geotechnical Journal 26:269–278.

[5] Fredlund, D.G., Rahardjo, H. (1995). Soil Mechanics for Unsaturated Soils. John Wiley and Sons, New York.

[6] Biot, M. A., and Willis, D. G. (1957). The elastic coefficients of the theory of consolidation, J. Appl. Mech., 24:594–601.

[7] Green, D. H., and Wang, H. F. (1990). Specific storage as a poroelastic coefficient, Water Resources Research, 26:1631–1637.

[8] Neaupane K.M., Yamabe, T. (2001). A fully coupled thermo-hydro-mechanical nonlinear model for a frozen medium. Computer and Geotechnics 28:613–637.

[9] Desai, C.S., Saxena, S.K. (1977). Consolidation analysis of layered anisotropic foundation, Int. J. Numerical and Analytical Methods in Geomechanics, 1:5–23.

[10] Lewis, R.W., Schrefler, B.A. (1989). Finite element method in the deformation and consolidation of porous media. Wiley, Chichester

[11] Tsaparas, I., Rahardjo, H., Toll, D.G., Leong, E.C., 2002. Controlling parameters for rainfall-induced landslides. Computer and Geotechnics, 29:1–2.

[12] Gasmo, J.M., Rahardjo, H., Leong, E.C., 2000. Infiltration effects on stability of a residual soil slope. Computer and Geotechnics, 26:145–165.

[13] Ng, C.W.W., Shi, Q. (1998). A numerical investigation of the stability of unsaturated soil slopes subjected to transient seepage. Computer and Geotechnics, 22:1–28.

[14] Gatmiri, B., Jabbari, E., 2005. Time-domain Green's functions for unsaturated soils. Part I: Two-dimensional solution. International journal of Solids and Structures 42 (23):5971–5990.

[15] Bishop, A. W. (1959). The principle of effective stress, Publication 32, Norwegian Geotechnical Institute, Oslo, Norway, 1–4.

[16] Bishop A.W., Blight, G.E. (1963). Some aspects of effective stress in saturated and partly saturated soils. Geotechnique, 13(3):177-197.

[17] Alonso E. E., Gens A., Josa A. (1990). A constitutive model for partially saturated soils. Geotechnique, 40(3): 405-430.

[18] Alonso E. E., Vaunat J., Gens A. (1999). Modeling the mechanical behavior of expansive clays, Engineering Geology, 54(1): 173-183.

[19] Jacquard, C. (1988). Etude experimentale dune barriere capillaire avec unmodele de laboratoire. PhD Thesis, CGI, Ecole Mines Paris. 165 pp.

[20] Lu, N., Likos, W.J. (2004). Unsaturated soil mechanics, Wiley, N.J.

[21] Bourgeois M (1986). Le concept de barriere capillaire. Etude par modele numerique. These, CGI, Ecole Mines Paris, pp133.

[22] Lloret, A., Alonso, E.E. (1985). State surfaces for partially saturated soils. In: Proc 11th Int. Conf. Soil Mechanics and Foundation Engineering, 12–16 August, San Francisco. Balkema, Rotterdam, vol 2, pp 557–562.

[23] Brun P. (1989). Cinetique d'infiltration au sein d'une couche d'argile compactee. Etude experimentale et numerique. PhD Thesis, ENSMP, Paris, pp 219.

[24] Noorishad, J., Tsang C. F. (1987). Thermal-hydraulic mechanical interactions in fluid injection into fractured rocks. Coupled processes associated with nuclear waste repositories (C.F. Tsang editors). Academic, Orlando, Fla.